Proceedings of the ASME 2010 3rd Joint US-European Fluids Engineering Summer Meeting and 8th International Conference on Nanochannels, Microchannels, and Minichannels
FEDSM-ICNMM2010
August 1-5, 2010, Montreal, Canada

FEDSM-ICNMM2010-31047

MODELING THE FORCES EXERTED ON THE TOOL-ELECTRODE DURING SPARK ASSISSTED CHEMICAL ENGRAVING CONSTANT VELOCITY FEED-DRILLING

Jana Abou Ziki
Concordia University
Department of Mechanical and Industrial Engineering
1455 de Maisonneuve Blvd. W.
Montreal, Quebec, Canada

Nand Kishor M. Dhawale
Concordia University
Department of Mechanical and Industrial Engineering
1455 de Maisonneuve Blvd. W.
Montreal, Quebec, Canada

Rolf Wüthrich
Concordia University
Department of Mechanical and Industrial Engineering
1455 de Maisonneuve Blvd. W.
Montreal, Quebec, Canada

ABSTRACT

Spark Assisted Chemical Engraving (SACE) is an interesting technology for micro-machining several types of non-conductive materials like glass, quartz, polymers and some ceramics.

The process takes place in an electrochemical cell with two electrodes immersed in an electrolyte. The electrolytic solution is typically sodium hydroxide (30%wt NaOH) or potassium hydroxide (KOH). The cathode is used as tool and the anode as counter-electrode.

When the applied voltage is higher than a critical value (typically around 30V, depending on the electrolyte and tool-electrode geometry) bubbles grow so dense on the electrode surface that they coalesce into a gas film. Electrical discharges occur between the electrode and the electrolyte. Machining begins consequently if the electrode is placed close enough to the surface to be machined (typically 25µm for glass).

In the present paper, the forces exerted on the tool-electrode during constant velocity feed drilling is investigated experimentally and a model is proposed. The setup is composed of a machine head mounted on XYZ precision linear stage holding the tool-electrode. The machining head further incorporates a force sensor which is able to monitor, during drilling operation, the force exerted on the tool-electrode based on the zero displacement measurement principle.

INTRODUCTION

Spark Assisted Chemical Engraving is a non-traditional micro-machining technology based on electrochemical discharge phenomena, first introduced by Kurafuji and Suda [1], that is used during glass micromachining [2]. Glass micro-machining was the first application and remains so far the best mastered technique even though other non-conducting materials can also be machined (e.g., granite, refractory fire-brick, aluminium oxide, plexiglass, quartz) [3]. Similar results are reported for ceramic materials [4] and quartz [5].SACE can be used for micro-hole drilling, 3D machining, travelling wire machining and hybrid techniques. The glass sample to be machined is dipped in the electrolyte (typically 30%wt NaOH) and a voltage is applied between the tool electrode (cathode) and the counter electrode (anode). The two electrodes are separated from each other and the tool electrode has smaller surface area than the counter electrode (Fig.1).

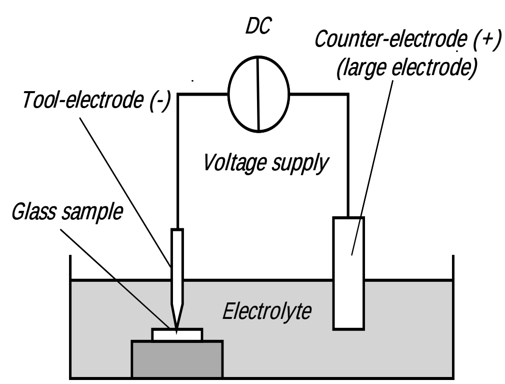

Fig 1.SACE MACHINING CHAMBER

As a voltage is applied between the electrodes, bubbles start to form around. When the voltage reaches a value slightly above the critical voltage (Fig.2) of 30 V, the number of growing gas bubbles is high enough in order to allow them to coalesce into a gas film, isolating the tool electrode from the electrolyte. The high electric field created in the film cause electrical discharges between the tool electrode and the electrolyte.

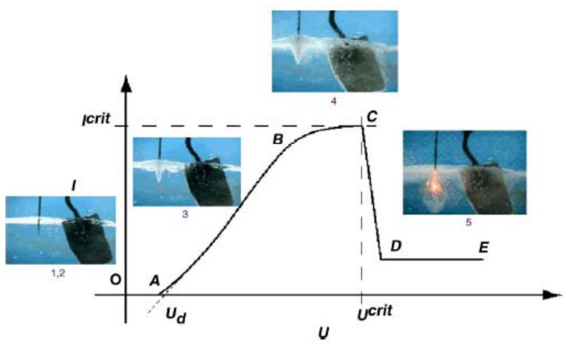

Fig 2.GAS FILM FORMATION AS A FUNCTION OF THE APPLIED VOLTAGE

Drilling is characterized by two regimes (Fig.3) [6]. During the discharge regime in the first 100-200 microns drilling depth the drilling is fast (up to 100microns/s) and controlled by the number of discharges (applied voltage). For higher depth, drilling becomes slower (typically around 10-15 microns/s) and is nearly independent of applied voltage, this behavior occurs during the hydrodynamic regime.

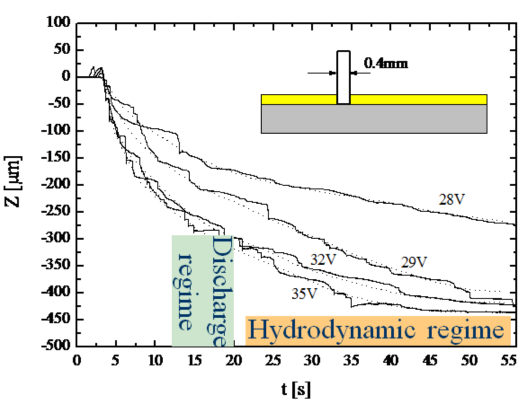

Fig 3.DISCHARGE AND HYDRODYNAMIC REGIMES

The low dependence of the material removal rate from the machining voltage at high depths is due to the difficulty for the electrolyte to flow inside the micro-hole and remove the machined material (Fig.4).

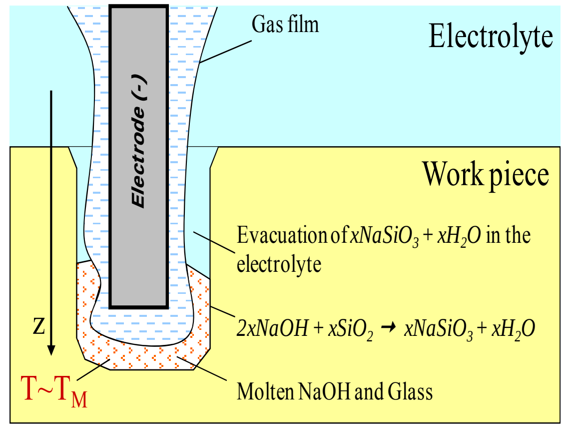

Fig 4.CHEMICAL REACTIONS AND TEMPERATURE IN THE MACHINING ZONE

The material removal mechanism is currently believed to be a combination of thermal and chemical effects [7]. The heat generated by the electrochemical discharges raises the temperature in the machining zone to about 500-600°C [7, 8]. At these high temperatures the electrolyte is in form of molten NaOH. The alkaline solution attacks the glass and is hydrated and totally dissolved by breaking the Si-O-Si bond on the surface of the glass:

$$OH^- + \equiv Si - O - Si \equiv \rightarrow \equiv SiO^- + \equiv SiOH \qquad (1)$$

This process is known as chemical etching and occurs according to the following equation:

$$2xNaOH + xSiO_2 \rightarrow xNa2\ SiO_3 + xH_2O \qquad (2)$$

The product of this reaction will be removed by the electrolyte outside the machining zone.

During the SACE drilling process, the tool will face a zone of viscous medium (high temperature glass and molten NaOH). If the tool evolution in the viscous material is modeled as a spherical object, Eq. (3) holds between the tool-drilling speed v and the force F pushing on it:

$$v = \frac{F}{6\pi\eta} \qquad (3)$$

with η the viscosity of the heated material.

Using the experimentally found limiting speed, which is around 1.5µm/s during gravity-feed drilling, and Eq.(1), the viscosity of the material in the machining zone was estimated to be $\eta = 1.4 \times 10^8\, Pa.s$ [8]. This viscosity corresponds to a temperature of the glass of around 600°C, which is less than the softening Littleton point provided by the microscope slides producer (720°C).

It is believed that micromachining of glass is not only caused by thermal effects but also by chemical etching because the material removal rate differs when different electrolytes are used [9-11]. NaOH electrolyte seems to have the most interesting properties compared to other electrolytes (KOH, NaCl, $NaNO_3$, NaF, HCl and H_2SO_4), especially for glass and quartz [1, 3, 10], and also for ceramics [12].

Till now no detailed analysis of the forces exerted on the tool-electrode has been given. However, a correlation between the machining current (current between electrodes) and the force exerted on the tool electrode while performing 2D- micro channels has been found [13]. It has been noticed that typically each 2 seconds the gas film break which lead to the observation of a current peak. This causes a tool-tip oscillation and thus a larger compensating force is needed to be provided by the controller.

It is important to know the origin of forces appearing on the tool tip so that a better control of the micro machining process could be achieved. Knowing the origin of these forces will result in deeper understanding of the machining process so that smoother micro holes with a better surface quality can be obtained.

In the present work, a model for interpreting the forces measured during constant velocity feed drilling is proposed. Validation is done through experiments.

EXPERIMENTAL SETUP

The overall setup consists of XYZ platforms (Cartesian robot) from NEWPORT. The SACE machine head assembly (Fig.5, 6) is mounted on the Z-axis of the XYZ stage. The work-piece is placed inside a processing cell mounted on the XY axes in order to align the work-piece relatively to the tool electrode. The used electrolyte was 30%wt NaOH prepared from deionized water. The work-pieces were standard microscope glass slides purchased from VWR International.

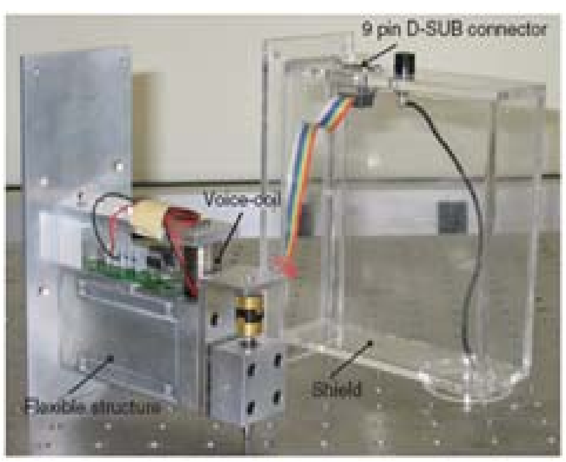

Fig 5.SACE MACHINE HEAD ASSEMBLY

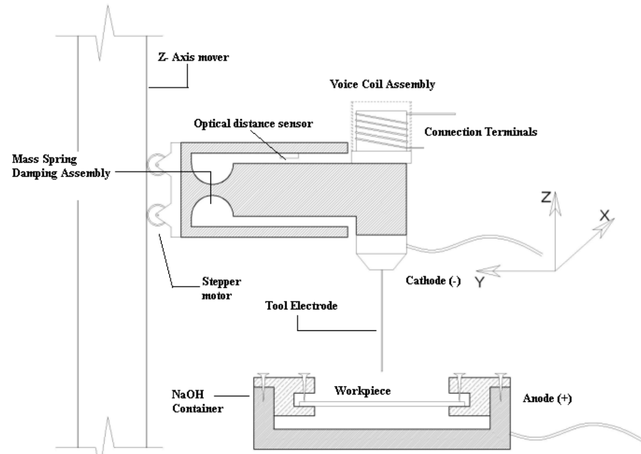

FIG 6.OVERVIEW OF SACE MACHINING SET-UP

The tool electrode, a stainless steel cylinder of 0.5 mm diameter, is connected to the machine head which is composed of a flexible structure (Fig. 6). The flexible structure can move upwards or downwards in the z direction. The machining head contains a PCB mounted position sensor with signal conditioning circuit and a voice coil actuator driven by a V/I converter unit. A computer system connected to a dSPACE 1104 controller board is used to control the machining head and to record the desired signals.

The force acting on the tool electrode is measured using the zero displacement principle. The relative distance between the flexible structure and its base is detected with an optical sensor. The optical sensor shows a linear response in the range of 0-700 microns and gives an output voltage in the range of 0.24-5.00V respectively. The position sensor value is fed to an Analog input channel of the dSPACE board. The relative distance between the flexible structure and its base is kept constant by a PID controller.

The controller is implemented with a simulink model where the dSPACE real time interface blocks are used. The zero- displacement measurement principle is used during experiments because it is so important for the constant velocity feed drilling. During constant velocity feed drilling, the tool electrode moves with a constant pre-set velocity and at the same time the distance between the work-piece and the tool-electrode should be kept constant. The zero displacement measurement principle allows the measurement of the force exerted on the electrode. Then the voice coil actuator is controlled to provide a force $F^{voice\text{-}ccoil}$ on the tool electrode that is opposite and equal to the force exerted on the tool electrode during machining (Fig.7).

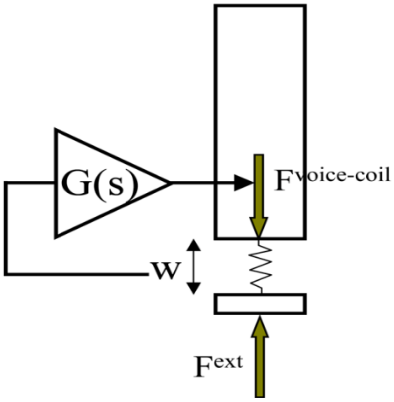

Fig 7.FORCES EXERTED ON THE TOOL-ELECTRODE DURING MACHINING. $F^{voice-ccoil}$ IS THE FORCE PROVIDED BY THE VOICE COIL ACTUATOR IN ORDER TO BALANCE THE FORCE F^{ext} EXERTED ON THE TOOL DURING DRILLING OPERATIONS TO KEEP *w* CONSTANT.

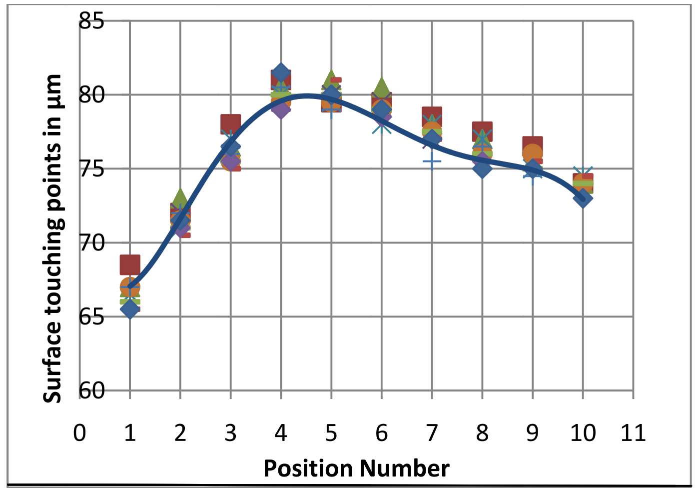

Fig 8.REAPEATABILITY FOR SURFACE TOUCHING AT 10 DIFFERENT POINTS ON WORK-PIECE

TESTING AND CALIBRATION

The sensor output has a good sensitive and linear region between 400-1150 µm of the flexible structure displacement. However, only a part of this range was used to control the voice coil actuator. After experimenting, the flexible structure position at 350 microns is chosen to be the initial position and the position corresponding to 750 microns (somewhere in between the working range) is considered the final position.

Pieces of pre-measured mass were used for calibration. Different masses were placed on the top space of the flexible structure. For each mass added, the signal from the sensor changes and the controller output changes to compensate for the error until it minimizes it to zero. The amount of force provided by the voice coil actuator for each mass placed is found to be equal and opposite to the force exerted by each mass on the flexible structure. The response time for the controller to compensate for the error was below 0.1 second.

The repeatability of machining setup was tested by moving the tool-electrode downwards to touch the glass at the same position several times. Figure 8 shows the results of an experiment of 10 iterations (out of 36) for 10 same positions on the work-piece. It is observed that the repetition of the setup for work piece surface touching with respect to each position is good, though variations from position to position are still present due to the presence of a minor deflection in work-piece. This variation is in agreement with the deflection resulting from the bending of the glass slide as calculated by the deformation of two side supported beam. However, the magnitude of the variation is very small compared to the value of deflection of the work-piece that is maximum in the middle and that is equal to83µm. Figure 8 shows that the repeatability for 10 iterations within same position is about 4 µm and the bending of the work piece is about 15 µm at the central position of the work-piece.

MODEL OF THE DRILLING FORCE

For the interpretation of the force measurements during drilling, the following model is proposed (Fig. 9).

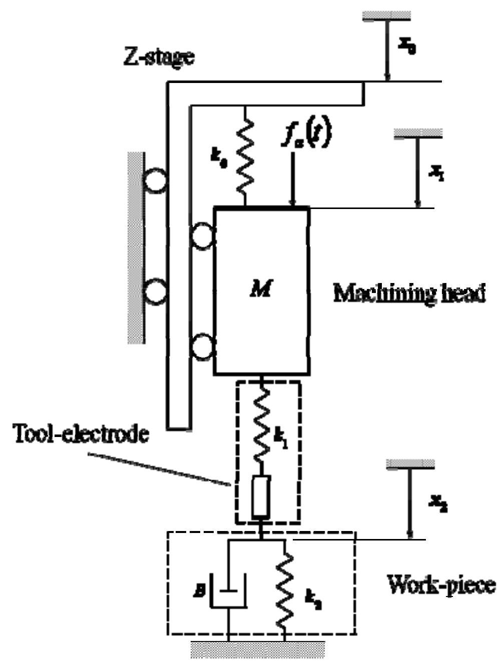

Fig 9.MECHANICAL MODEL OF THE SYSTEM: k_1, k_2 AND B ARE THE STIFFNESS OF THE TOOL-ELECTRODE , STIFFNESS OF THE WORKPIECE AND THE DAMPING DUE TO VISCOUS MATERIAL IN FRONT OF THE TOOL-ELECTRODE RESPECTIVELY. $x_1(t)$, $x_2(t)$ AND $f_a(t)$ ARE THE DESIRED MOTION OF THE TOOL-ELECTRODE FIXATION, THE TOOL-ELECTRODE TIP COORDINATE, AND THE FORCE OF THE VOICE-COIL ACTUATOR PUSHING ON THE TOOL-ELECTRODE RESPECTIVELY.

The machining head of mass M is mounted on the Z-stage of coordinate $x_0(t)$. The force $f_a(t)$ is the force pushing on the tool such that the desired motion $x_1(t)$ of the tool-electrode fixation can be achieved. In the following it will be assumed that the controller of the machining head is ideal, such that $x_1(t) - x_0(t)$ is constant. Therefore the spring k_0, modeling the stiffness of the flexible structure of the machining head, does not enter into the force balance. The position $x_2(t)$ is the tool-electrode (the mass of which is neglected here) tip coordinate. The stiffness of the tool-electrode and its fixation are modeled by the spring k_1.

The force exerted on the tool-electrode is represented by a spring dashpot parallel combination where the spring k_2 is the stiffness of the work-piece and the dashpot B is modeling the viscous material in front of the tool-electrode [7].

The Kelvin–Voigt model is used to represent the force exerted on the tool electrode in order to model reversible, visco-elastic strain. Upon application of a constant stress, the material deforms at a decreasing rate, asymptotically approaching the steady-state strain. When the stress is released, the material gradually relaxes to its undeformed state. At constant stress (creep), the model is quite realistic as it predicts strain to tend to σ/E as time continues to infinity.

Note that in case the machining voltage is switched off, the damping is equal to zero ($B = 0$). The parallel combination of these two elements is motivated by the fact that the gas film is instable and periodically has to be reformed [14]. Consequently, the tool-electrode is periodically pushing on the work-piece or the viscous material in front of the tool depending on the presence or not of the gas film. The spring constant k_2 can be estimated, in case the work-piece is supported at its two extremities (supposing the stiffness of the mounting assembly is much larger than the one of the work-piece), by:

$$k_2 = \frac{L^3}{48EI} \tag{4}$$

with L the length ($L = 76 \cdot 10^{-3}$ m), E the modulus of elasticity ($E = 65 \cdot 10^9$ N/m^2) and I the moment of inertia ($I = 2.1 \cdot 10^{-12}$ m^2) of the work-piece. In the used experimental set-up, the value of k_2 is $k_2 = 1.5 \cdot 10^4$ N/m. The dashpot damping coefficient B can be estimated, based on Stock's law of viscous friction, as [7]:

$$B = 6\pi\eta r \tag{5}$$

with η the viscosity of softened zone in front of the tool-electrode and r the radius of the tool-electrode. Using the estimation of $\eta = 1.4 \cdot 10^8$ Pa $\cdot$ s from Jalali et al. [7], it follows that $B = 3.5 \cdot 10^5$ N $\cdot$ s/m.

For this proposed model, the equations of motions write:

$$M_1 \ddot{x}_1 = k_1(x_2 - x_1) + f_a(t) \tag{6}$$

$$B\dot{x}_2 = k_1 x_1 - (k_1 + k_2)x_2 \tag{7}$$

In the present study, the case of constant velocity feed drilling is considered:

$$x_1(t) = vt \tag{8}$$

with v the imposed drilling speed.

Note that it is assumed that the controller of the force sensor (zero displacement force measurement) is ideal, i.e. its response time is neglected. Solution of Eq. 0-0 is:

$$x_2(t) = \frac{k_{eq}}{k_2} v\left[t + \tau\left(e^{-t/\tau} - 1\right)\right] \tag{9}$$

with

$$k_{eq} = \frac{k_1 k_2}{k_1 + k_2} \tag{10}$$

the equivalent stiffness (stiffness of the system when machining voltage is switched off) and the typical time constant is:

$$\tau = \frac{B}{k_1 + k_2} \tag{11}$$

Since the driving force $f_a(t) = k_1(x_1 - x_2)$ exerted by the voice coil, it follows

$$f_a(t) = k_{eq}\left[t - \tau\frac{k_1}{k_2}\left(e^{-t/\tau} - 1\right)\right] \tag{12}$$

Figure 10 shows the plot of the force exerted on the tool-electrode with respect to time.

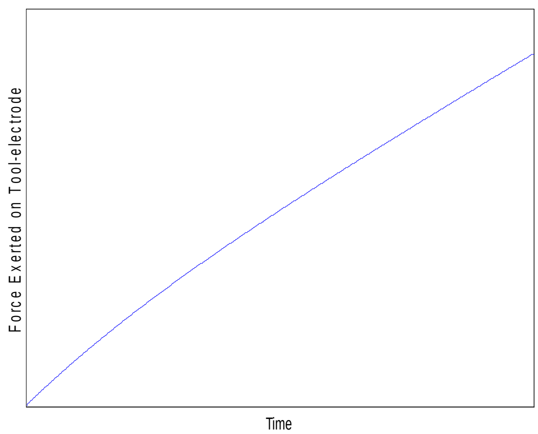

Fig 10.PLOT OF FORCE EXERTED ON TOOL-ELECTRODE AS A FUNCTION OF TIME

Equation (12) represents the model of the force exerted on the tool-electrode during machining at constant velocity feed (Fig.10). First the force starts to grow with a slope k_1 compared to x_1:

$$f_a(t) = k_1 vt \text{ , for } t \to 0 \tag{13}$$

before reducing its grow rate to k_{eq} :

$$f_a(t) = k_{eq} vt + \left(\frac{k_{eq}}{k_2}\right)^2 Bv \text{ , for } t \to \infty \tag{14}$$

As one has $x_1(t) = vt$, one can as well write the last two equations in function of the drilling depth x:

$$f_a(x) = k_1 x \text{ , for } \quad x \le \xi \tag{15}$$

and

$$f_a(t) = k_{eq} x + \left(\frac{k_{eq}}{k_2}\right)^2 Bv \text{ , for } \quad x > \xi \tag{16}$$

with $\xi = v\tau$ the characteristic depth.

RESULTS AND DISCUSSION

The following experiments are conducted. In the first experiment, the tool-electrode is positioned at a fixed height above the work-piece surface (about 40 microns in the case shown). This height is the zero position of the z axis and it is indicated in (Fig.11) as 0 microns.

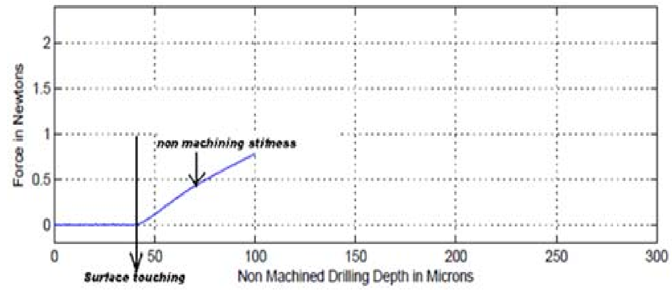

Fig 11.PLOT FOR DETECTION OF SURFACE TOUCHING

The tool electrode is then moved down along the z axis, while the machining voltage was switched off, till it touches the glass surface. As shown in (Fig.11), the force exerted on the tool electrode was zero at depth less than 40 microns before increasing indicating that the electrode touched the glass. The slope of the straight line is the stiffness of the electrode and the glass surface.

After identifying the stiffness, the experiment is repeated while the machining voltage is switched on. As shown in (Fig. 12), the force is detected at depth equal to 20 microns, which is earlier than in the first case. It is noticed that first the force increased with a high slope in agreement with Eq. (15). Then the slope became less inclined, as predicted by Eq. (16), before going back to zero. This vanishing is attributed to the fact that after certain time the electrolyte is able to enter the hole and remove the molten NaOH resulting in zero force on the tool electrode. This scenario is then repeated, depending on cases, several times.

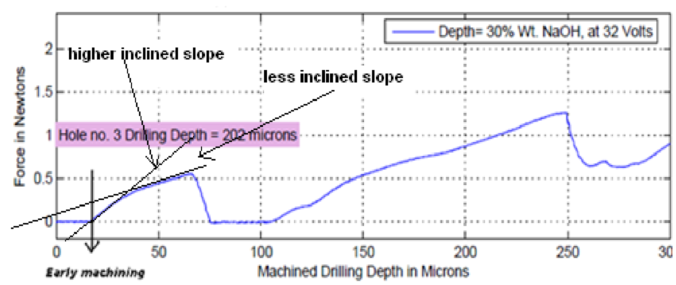

Fig 12.PLOT OF FORCE VS. MACHINING DRILLING DEPTH

The graph shows repeated patterns but the slopes of the curve slightly change as machining proceeds due to the fact that at higher depths it is harder for the electrolyte to enter the hole. Consequently, machining will switch to the hydrodynamic regime resulting in bigger forces on the tool electrode.

As shown in (Fig.11, 12), during drilling operations the force is detected earlier than in dry experiments.

Possible reasons for the appearance of this force may be:

- thermal expansion of the tool-electrode and the work-piece
- pressure due to bubble evolution and gas film formation resulting in pushing the tool
- formation of a molten NaOH layer on the work-piece

Thermal Expansion of the Tool-electrode and the Work-piece

The distance from the initial position of the tool electrode, before the machining starts, to the position at which a force is sensed is plotted as a function of the machining voltage for different machining voltages (Fig.13).

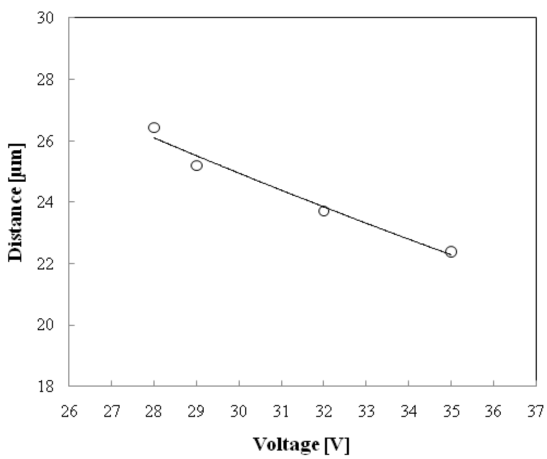

Fig 13.DISTANCE BETWEEN THE TOOL-ELECTRODE TIP AND THE GLASS SURFACE AS A FUNCTION OF THE APPLIED VOLTAGE

With increasing machining voltage the local temperature increases resulting in increasing the thermal expansion of the tool-electrode and work-piece and thus force is detected at smaller distances.

If this is the case, then the tool electrode must expand by 25 microns in order to explain the results of (Fig.11, 12). However, if the change in length of the tool-electrode, made of a stainless steel cylinder dipped in the electrolyte about 500 microns, is calculated using the linear thermal expansion equation, only an expansion of about 5 microns results.

Further, (Fig.13) shows that as the machining voltage increases, the distance at which a force is sensed decreases. It should be noted that the difference in the distance with the change in voltage is only few microns (about 5 microns). This trend is opposite to what would be expected if thermal expansion is responsible for the early force detection (the higher the voltage, the hotter will be the tool-electrode).

Therefore it is concluded that the thermal expansion of the tool-electrode and the work-piece is not likely to contribute much to the early appearance of the force.

Pressure Due to Bubble Evolution and Gas Film Formation Resulting in Pushing the Tool

To further investigate this hypothesis, the following experiment was conducted. Prior to machining, the tool-electrode is positioned at a given height Δz above the work-piece. Machining voltage is then switched on. While moving the tool-electrode towards the glass surface, the average force exerted on the tool-electrode during machining is plotted as a function of delta z which is the distance between the tool electrode and the work piece (Fig.14).

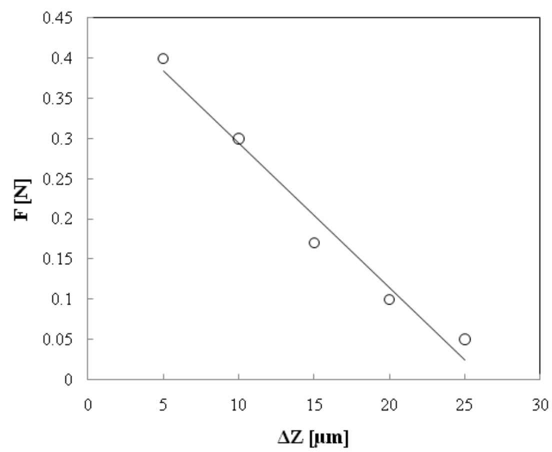

Fig 14.FORCE EXERTED ON THE TOOL-ELECTRODE TIP AS A FUNCTION OF THE DISTANCE SEPARATING THE TOOL-ELECTRODE AND THE GLASS SURFACE

Figure 14 shows, that when the distance Δz between the tool-electrode and the glass surface is less than 25 microns, the force exerted on the tool electrode increases as Δz decreases. It is concluded from (Fig.14) that the distance between the tool-electrode and the work-piece must be higher than 25 microns to obtain negligible force acting on the tool-electrode during micro-machining. This is in agreement with previous observations showing that a maximal distance of 25 µm between tool-electrode and work-piece is allowed in order for the machining to take place [15].

The origin of this force may be explained by the fact that while applying a voltage between the electrodes, bubbles start forming around the tool electrode eventually coalescing into a gas film which exerts an upward pressure on the tip of the tool electrode. The gas film mean life-time is typically in the order of a few tens of milliseconds [14].

However, considering that the tool-electrode used had a diameter of 0.4 mm and that the force exerted on the tool-electrode is equal to 0.4 N (Fig.14), for distance equal to 5 microns, the pressure in the gas film should then be equal to more than 30 atm, which is a very unlikely value.

Consequently, the origin of the force sensed when the machining voltage is switched on and the tool-electrode positioned above the glass surface, is unlikely to come solely from the pressure due to bubbles and the formation of the gas film. The following section proposes a more plausible explication of its origin.

Formation of a Molten NaOH Layer on the Work-piece

Due to the discharge activity across the gas film, the tool-electrode and its vicinity is significantly heated up (around 600°C [7] and [8]). As a result, the water inside the electrolyte surrounding the tool-electrode evaporates locally. Only NaOH remains, which is most likely in a molten state (NaOH melting point: 318°C and boiling point: 1390°C). In the narrow gap between the tool-electrode and the work-piece, a layer of molten NaOH will be formed as shown in (Fig.15). Because the density of this layer is much higher than the water, the layer formed takes the shape shown in (Fig.15) and it exerts a force on the electrode. It is likely that this effect is at the origin of the early force detection effect.

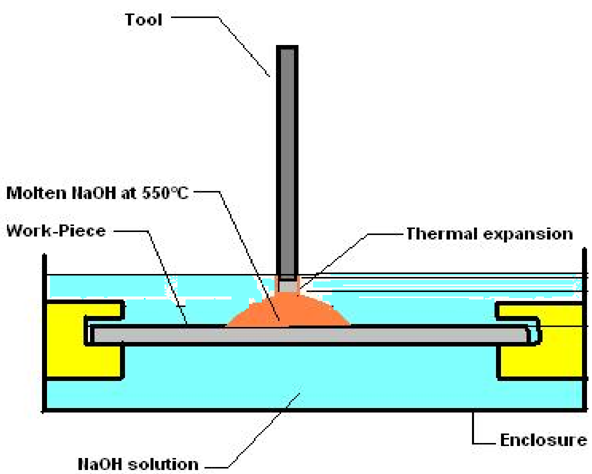

Fig 15. RISE IN THE WORK-PIECE SURFACE HEIGHT DUE TO THE DEPOSITION OF MOLTEN NAOH AFTER EVAPORATION OF WATER AND PARTIAL THERMAL EXPANSION IN TOOL

CONCLUSION

In this paper, a model for interpreting the forces acting on the tool-electrode during SACE machining process was presented. Further it was found that a significant force is acting on the tool-electrode even before touching the actual work-piece surface. Experiments were done to further investigate the origin of this early force detection. The results show that thermal expansion of the tool-electrode and the work piece, pressure due to the gas film formation and the formation of a molten NaOH layer under the tool-electrode tip are the main factors contributing to the appearance of the early force.

Machining with the knowledge of the origin of the forces acting on the tool-electrode will enhance the understanding of the SACE machining process. This will eventually allow the application of closed-loop SACE machining using force-feedback methods targeting to increase the accuracy as well as the repeatability of SACE machining process. The current force investigation will give a great shot for the on-going research in the field of glass micromachining using electrochemical discharge phenomenon which will allow the application of SACE in the production of functional and lab-on chip micro-devices.

ACKNOWLEDGMENTS

This work was supported by the Fonds québécois de la recherche sur la nature et les technologies.

REFERENCES

[1] Kurafuji, H., and Suda, K., 1968, "Electrical Discharge Drilling of Glass," Annals of the CIRP, 16pp. 415-419.
[2] Wüthrich, R., and Fascio, V., 2005, "Machining of Non-Conducting Materials using Electrochemical Discharge Phenomenon--an Overview," International Journal of Machine Tools and Manufacture, 45(9) pp. 1095-1108.
[3] Cook, N. H., Foote, G. B., Jordan, P., 1973, "Experimental Studies in Electro-Machining," Journal of Engineering for Industry-Transactions of the ASME, 96 pp. 945-950.
[4] Tokura, H., Kondoh, I., and Yoshikswa, M., 1989, “Machining a Glass Rod with a Lathe-Type Electro-Chemical Discharge Machine,” Journal of Materials Science, 24 pp. 991.
[5] Jain, V.K. and Chak, S.K., 2000, “Electrochemical Spark Trepanning of Alumina and Quartz,” Machining Science and Technology, 4 pp. 277-290.
[6] Wüthrich, R., Spaelter, U., Wu, Y., 2006, "A Systematic Characterization Method for Gravity-Feed Micro-Hole Drilling in Glass with Spark Assisted Chemical Engraving (SACE)," Journal of Micromechanics and Microengineering, 16(9) pp. 1891-1896.
[7] Jalali, M., Maillard, P., and Wüthrich, R., 2009, "Toward a Better Understanding of Glass Gravity-Feed Micro-Hole Drilling with Electrochemical Discharges," Journal of Micromechanics and Microengineering, 19(4) pp. 45001-45008.
[8] Jalali, M., Maillard, P., Mishra, S. P., Kadem, L., and Wüthrich R., 2007, “Modeling Gravity Feed Micro Hole Drilling by Electrochemical Discharge”, 2nd International Conference on Micro-Manufacturing, Greenville, South Carolina, USA
[9] Basak, I., 1991,″Electrochemical Discharge Machining Mechanism and a Scheme for Enhancing Material Removal Capacity,″ Ph.D. thesis, Indian Institute of Technology, Kanpur, India
[10] Yang, C. T., Ho, S. S., and Yan, B. H., 2001, "Micro Hole Machining of Borosilicate Glass Trough Electrochemical Discharge Machining (ECDM)," Key Engineering Materials, 196pp. 149-166.
[11] Didar, T.F., Dolatabadi, A., and Wüthrich, R., 2009, "Local Hardness and Density Variation in Glass Substrates

Machined with Spark Assisted Chemical Engraving (SACE)," Materials Letters, 63 pp. 51.

[12] Tsutsumi, C., Okano, K., and Suto, T., 1993, "High Quality Machining of Ceramics," Journal of Materials Processing Technology, 37(1-4) pp. 639.

[13] Wüthrich, R., Fascio, V.,Vinquerat D. and Langen H.,2000, “Study of Spark Assisted Electrochemical Etching - Force Measurements,” International Workshop on Microfactories (IWMF), Fribourg, pp.201-204.

[14] Allagui, A. and Wüthrich, R., 2009,"Gas Film Formation Time and Gas Film Life Time during Electrochemical Discharge Phenomenon", Electrochimica Acta, 54 pp. 5336-5343.

[15] Fascio, V., Wuthrich, R., Viquerat, D. and Langen, H., 1999, “3D Microstructuring of Glass Using Electrochemical Discharge Machining (ECDM),” Proc. of the International Symposium of Micromechatronics and Human Science, Nagoya, pp. 179-183.